Coordination octahedron distortion effect on x-ray absorption fine structures of titanium in the rutile titanium dioxide

1999 J. Phys.: Condens. Matter 11 1123

(http://iopscience.iop.org/0953-8984/11/4/020)

J. Phys.: Condens. Matter **11** (1999) 1123–1137. Printed in the UK PII: S0953-8984(99)91709-5

Coordination octahedron distortion effect on x-ray absorption fine structures of titanium in the rutile titanium dioxide

Valérie Jeanne-Rose† and Bertrand Poumellec

Université Paris Sud XI, Laboratoire de Thermodynamique et Physico-Chimie des Matériaux, Bâtiment 414 Centre d'Orsay, 91 405 Orsay Cédex, France

Received 16 February 1998, in final form 14 September 1998

Abstract. We have computed the x-ray absorption spectrum for the Ti K-edge in rutile titanium dioxide (TiO_2) in the frame of the multiple scattering approach, varying the atom positions within the coordination sphere. This allowed us to understand the origin of the absorption structure variation. The analysis has been achieved by making distortions of the axial and equatorial Ti–O distances or of the O_{eq}–$\hat{Ti}$–O_{eq} equatorial angle along the c axis. Computations are performed using FEFF (version 6) code for TiO_2 with Dirac–Hara and Hedin–Lundqvist exchange potentials. From the results, we can better understand why the amplitude of one or several structures is modified referring to TiO_2, when a variation of the local geometry occurs.

1. Introduction

Amongst the rutile family, the best known is titanium dioxide (TiO_2), because of its large industrial interest [1]. It is used in white pigment production in the paintwork domain (the most important), but also in paper, ceramic, textile or glass manufacture [2, 3] and also catalysis [4].

For these applications, it is useful to determine the local atomic arrangement around Ti. In this way, x-ray absorption structure (XAS) is a good tool as no long range order is required, but a good knowledge of the XAS is necessary.

Experimental determinations of the XAS absorption have been achieved by Grunes [5], Waychunas [6], Faisant [1], Poumellec *et al* [7] and Locock *et al* [8]. Beaurepaire *et al* [9] made a comparison between the Bremsstrahlung isochromat spectroscopy (BIS) and XAS absorption for TiO_2. Several authors compared different methods of calculation, for example, Kizler [10] discusses augmented plane wave (APW), linear muffin-tin orbital (LMTO) and multiple scattering (MS) methods to calculate the K-or L-edges of many systems and draws conclusions about their efficiency. De Groot *et al* [11], Zaldo *et al* [2] and Poumellec *et al* [12] calculated the titanium dioxide density of states (DOS) for rutile or anatase. Brydson *et al* [13] calculated the absorption cross section using the ICXANES code [14, 15] (multiple scattering method). Borgias *et al* [16] applied the same approach for titanium complexes. The titanium environment in these compounds exhibit some similarities to this one in rutile. The multiple scattering (MS) method appears the most efficient and as long as it is precise enough, we have used this one for our calculations.

Ruiz-López and Muñoz-Páez [17] and Borh *et al* [18] suggested an interpretation for the rutile and anatase TiO_2 XANES structures. They obtained a convergence for a cluster

† Current address: Université des Antilles et de la Guyane, Faculté des Sciences Exactes et Naturelles, Département de Chimie, BP 250, 97 157 Pointe-à-Pitre Cédex, Guadeloupe, France.

0953-8984/99/041123+15$19.50

containing 75 atoms and concluded that the absorption at low energies arises from a p–d titanium orbital mixing. Natoli *et al* applied recently the Continuum code with rutile TiO_2 [19–21].

Dufek *et al* [22] and Soldatov *et al* [23] studied another compound of the rutile family, manganese difluoride, using the multiple scattering method with a self-consistent potential.

For our purpose, the FEFF (version 6) code [24] has appeared more suitable for rutile TiO_2 absorption cross section calculations. With this code, it is easy to modify the initial geometry of the rutile (or also the kinds of atom) in order to understand the connection between the x-ray absorption and the atomic environment.

2. Rutile structure

Titanium dioxide crystallizes in the tetragonal rutile structure (space group $P4_2/mnm$ (D_{4h}^{14})) [25, 26].

The metal atoms (M, for example titanium) are at $(0, 0, 0)$ and $(0.5, 0.5, 0.5)$ and the neighbouring atoms B (oxygen) $(1 \pm u, 1 \pm u, 0)$ and $(0.5 \pm u, 0.5 \pm u, 0.5)$, where u is a constant having a value close to 0.3. The two M atoms (with the above positions) are equivalent by 90° rotation around the crystal c axis followed by a translation. The M atoms are located at the centre of a distorted octahedron forming an MB_6 cluster as indicated in figure 1. All of these octahedra form a rectilinear chain with the equatorial plane perpendicular between two consecutive chains.

Thus, there is a difference between the axial (d_a) distance (two apical distances of the octahedron), and the four equatorial MB distances (d_e). The latter is the distance to the four equatorial atoms in the basal plane of the octahedron, while the former is the apical distance joining the neighbouring and metal atoms. We can write for the rutile structure [27–29]

$$d_a = au\sqrt{2} \qquad \text{and} \qquad d_e = a\left[2\left(\frac{1}{2} - u\right)^2 - \left(\frac{c}{2a}\right)^2\right]^{1/2}$$

where a and c are unit crystallographic vector values.

Moreover, the equatorial atoms B make two angles θ_{eq1} and θ_{eq2} shown in figure 2 such that:

$$\theta_{eq1} + \theta_{eq2} = \pi \qquad \text{and} \qquad \theta_{eq1} < \pi/2.$$

The lattice parameters of TiO_2 were studied by several groups [17, 29–32]. We used the measurements of Blanchin and Vicario [30] and Cromer and Hernington [32]; these values are summarized in table 1.

Table 1. Structural parameters for TiO_2 in the rutile structure (distances are in Å and angle θ in degrees).

a, b	4.594
c	2.958
u (internal)	0.305
d_e	1.946
d_a	1.984
θ_{eq}	81.06

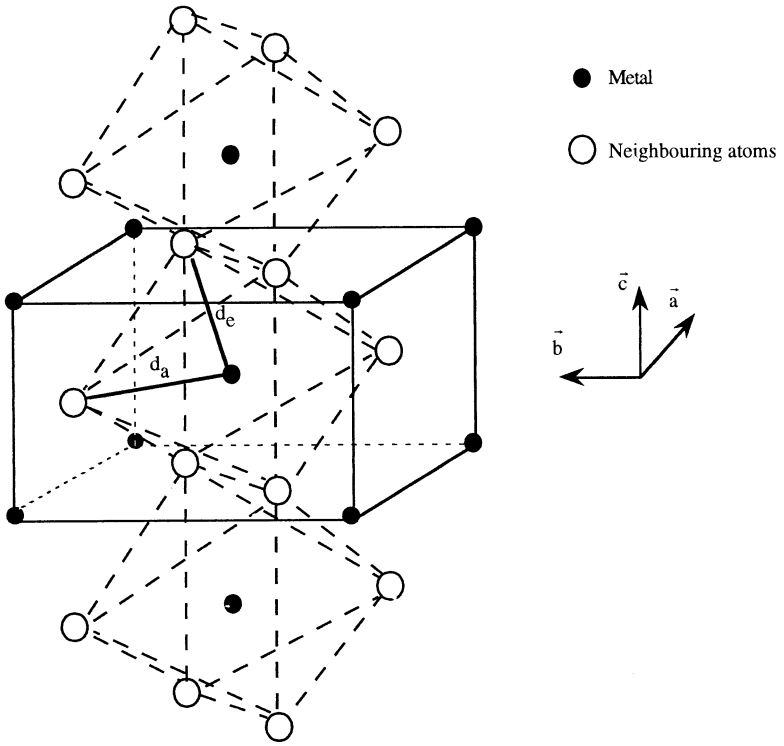

Figure 1. Crystallographic structure of rutile compounds where the metal atom is titanium and the neighbouring atoms are oxygen.

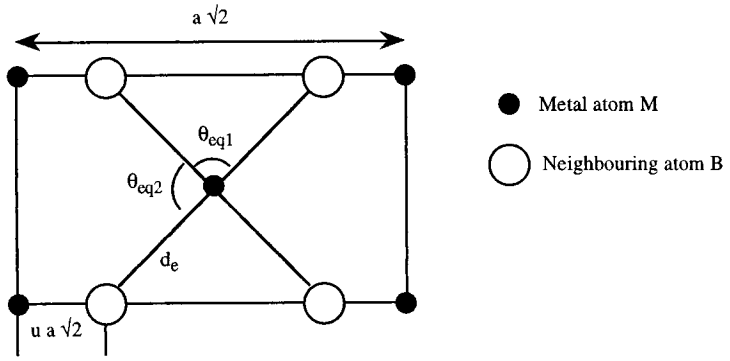

Figure 2. Plane (110) in the rutile structure showing the equatorial angles θ_{eq}, where the metal atom is titanium and the neighbouring atoms are oxygen.

3. Computations

3.1. The multiple scattering method, calculation details

Brydson *et al* [13] calculated the absorption of TiO_2 (rutile and anatase phases) with the ICXANES Code. Dagg *et al* [33] computed the absorption with ICXANES [14, 15] and MUFPOT. This last code computes the phase-shift in the one electron approximation with

fundamental state electron configuration. We made also computations using the ICXANES code, but in this paper, we present only some results performed with the FEFF (version 6) code [24]. The phase-shifts in this case are obtained in the excited state. Although FEFF has this advantage over ICXANES, this code is unable to reproduce correctly the absorption for low energies. In addition, the appearance of a non-zero absorption for energies below the Fermi level is due to the fact that the Green method used in the calculation [34] does not take into account the occupancy of the states. This is overcome by using an arctan function here; this does not correct the pre-edge intensity enough which remains too strong.

The FEFF6 code performs a multiple scattering approach and makes a path analysis with four modules. This program calculates the atomic potential for isolated atom and considers a different potential for the absorbing and neighbouring atoms of a given type. The configuration is neutral for the central atom with a $Z + 1$ charged nucleus; it takes into account a core hole. The other atoms are in the fundamental state [24]. The scattering potentials are calculated with an overlapping of the atomic potential using the muffin-tin approximation. The comparisons between exchange potentials are reported: the Dirac–Hara (D–H) potential is real and dependent on the energy and the Hedin–Lundqvist (H–L) potential is complex and dependent on the energy; its imaginary part takes into account the intrinsic losses due to plasmon coupling [35]. The muffin-tin radius is determined by the Norman criterion. The potential and the charge density are calculated according to the Loucks method [24, 36]. The electron mean free path is determined from the imaginary part of the photoelectron potential and allows us to take into account the intrinsic losses. Afterwards, the code determines the contribution from each path in the plane wave approximation and calculates again these contributions but in the curved wave approximation [35, 37]. The result of the procedure is the determination of the main significant paths [38].

3.2. Description of the model

The cluster used for our model contained 11 titanium and 14 oxygen atoms in a sphere with a radius of 3.56 Å. The values taken into account are according to the crystallographic orientation given by Blanchin and Vicario [30] and Cromer and Hernington [32]. See section 2 and table 1. A maximum pathlength of 16 Å was used with multiple scattering.

4. Results from FEFF6 code and comparison with the experiment

4.1. Experimental section

The experimental x-ray absorption spectra for both polarizations (parallel and perpendicular to the *c* axis) were recorded at LURE-DCI (Laboratoire pour l'Utilisation du Rayonnement Electromagnétique: 1.85 GeV, 260 mA, EXAFS II beam line [39]) at Orsay (France) under linearly polarized light.

Normalization was achieved by extrapolating the atomic cross section near the edge from the one estimated in the EXAFS region. The total process of this experiment is detailed elsewhere [7].

4.2. Results obtained with different potentials and comparisons

We used the Dirac–Hara (D–H) and Hedin–Lundqvist (H–L) exchange potentials. Our results are in good agreement with the experiment, for the polarizations either parallel (figure 3) or perpendicular to the *c* axis (figure 4). To compare correctly the spectra (the amplitude of the XANES and EXAFS structures and the positions of the maxima), the calculated absorption

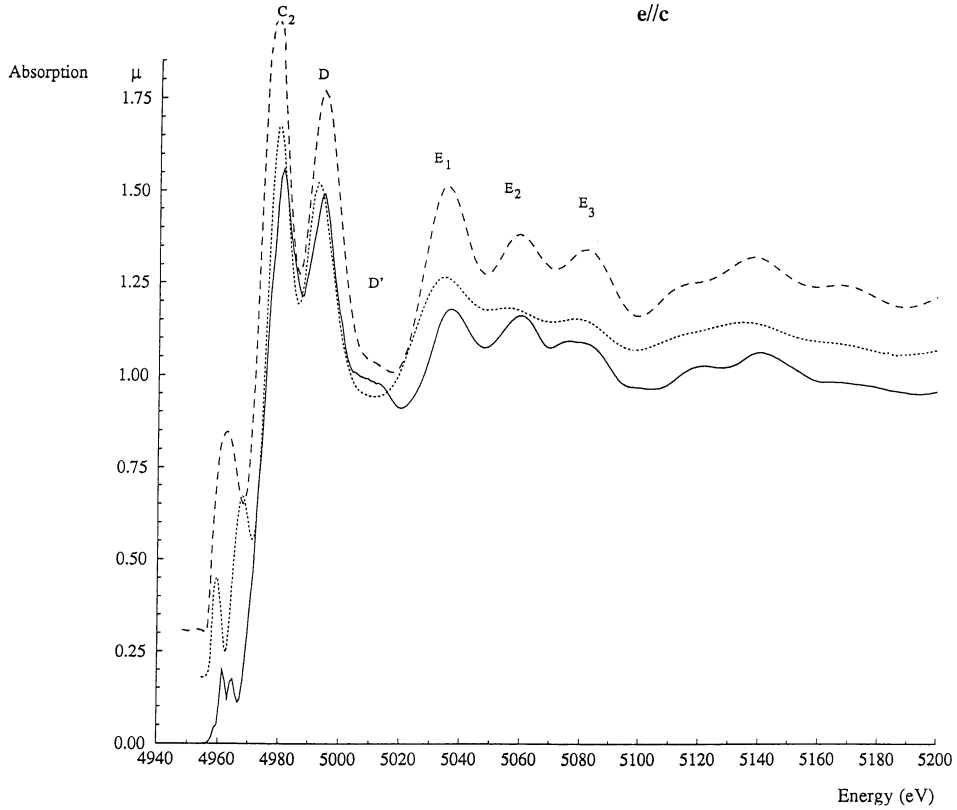

Figure 3. Comparison between the calculated absorption and the experiment for rutile TiO_2, with polarization parallel to the *c* axis. Solid line: experimental spectrum. Dotted line: absorption calculated using a Hedin–Lundqvist (H–L) exchange potential. Dashed line: absorption calculated using a Dirac–Hara (D–H) exchange potential.

has been shifted along the absorption axis. We remark that the amplitude of the XANES structures C_2 and D are too large when the D–H exchange potential is used (figure 3). D′ is reproduced only with the D–H potential; the EXAFS structures are not strong enough with the H–L potential. This is due to the electron mean free path which yields too strong dumping. For this potential, we cannot reduce the dumping in increasing the photoelectron mean free path because it has already a maximum value (no imaginary part in H–L potential). For the other case (D–H), we may increase the dumping for a better agreement with the EXAFS structures but in this way the D′ structure vanishes.

The same observations and remarks can be made for the polarization perpendicular to *c* (figure 4). All the peaks are reproduced, except the peak named C_1 (experimental absorption, solid line in figure 4).

It is worth noticing that we performed many tests and computations to try to obtain this structure [40]: for example, to increase the number of atoms included into the cluster, the two oxygen atoms (axial and equatorial) have been considered different in the calculation of the potential; we tested also the overlapping potential effect.

We think that the absence of C_1 is not the result of a broadening but this comes from the calculation of the potential. Soldatov *et al* [23] obtain the two structures C with a self-consistent potential in the excited state. Brydson *et al* [41] in studying the absorption of Be in BeO_4

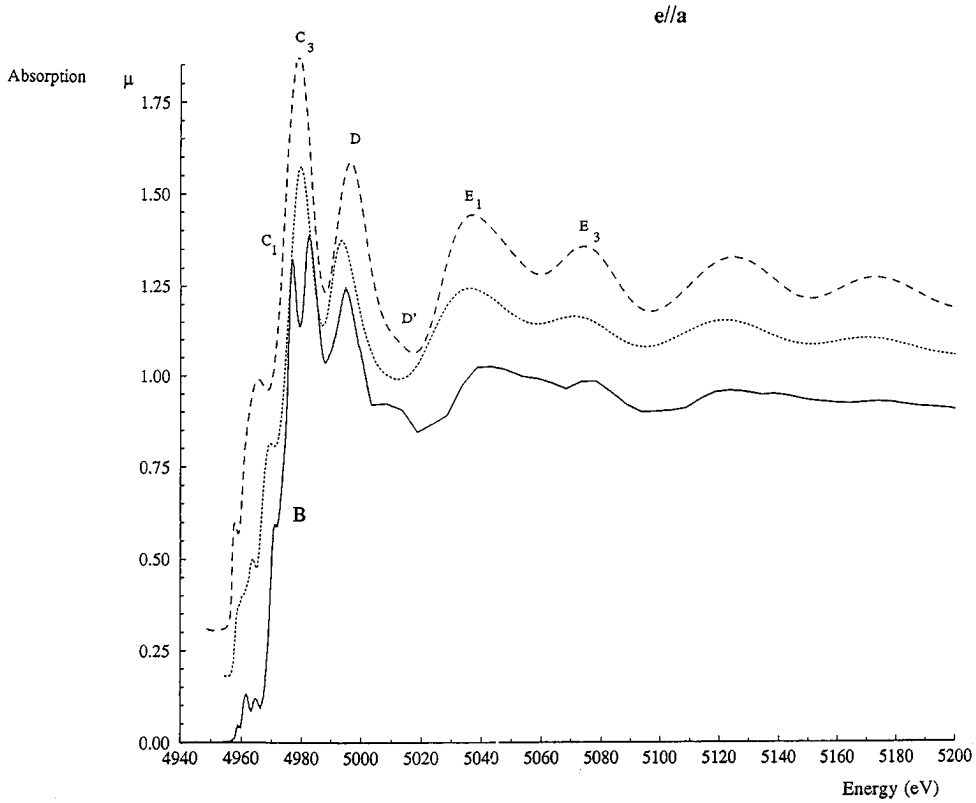

Figure 4. Comparison between the calculated absorption and the experiment for rutile TiO_2, with polarization perpendicular to the *c* axis. Solid line: experimental spectrum. Dotted line: absorption calculated using a Hedin–Lundqvist (H–L) exchange potential. Dashed line: absorption calculated using a Dirac–Hara (D–H) exchange potential.

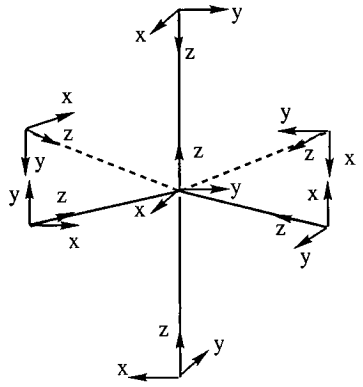

Figure 5. Atom displacement directions according to the local axis orientation.

(structure close to rutile) showed for this compound that the spectra exhibit a double peak only with a self-consistent potential. In our case, the FEFF6 code used the $Z + 1$ approximation but the potential is not really self-consistent. Although it is a good approximation of the

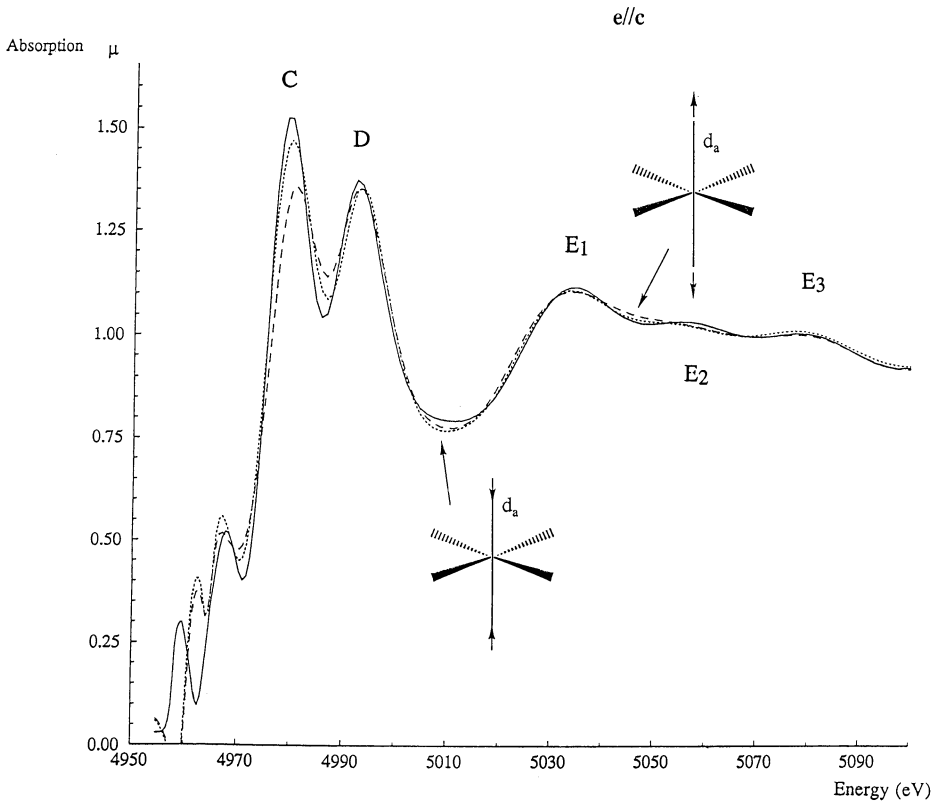

Figure 6. Calculated absorption of rutile TiO_2, with polarization parallel to the *c* axis. Solid line: rutile TiO_2 without distortion. Dotted line: reduction of the axial bond lengths. Dashed line: increasing of the axial bond lengths.

self-consistent field in the LDA (local density approximation) [38], the non-consistency may be the cause for C_1 to be missing. Finally, in our laboratory, Aïfa *et al* [42, 43] calculated the absorption of TiO_2 in order to interpret the pre-edge fine structures (PEFS) of the Ti K-edge of rutile titanium dioxide in the frame of multiple scattering with the muffin-tin approximation. They use a new code from the Department of Physics in Rostov (XAFS-Rostov). The potential inside atomic spheres is calculated by the Herman–Skillman procedure [44] (self-consistent). Electron configurations for all non-absorbing atoms are those for neutral free atoms. The electron configuration for the absorbing atom takes into account the core hole and screening charge existence. In that case, the authors obtain a double peak C_1–C_3 for the polarization $e \perp c$.

Nevertheless, for our calculations, we can conclude that the Hedin–Lundqvist exchange potential reproduces better the XANES structures, whereas the Dirac–Hara exchange potential in FEFF6 reproduces better the experimental spectrum in the EXAFS region.

Therefore, for all geometry distortion calculations, we have used the Hedin–Lundqvist exchange potential for a cluster of 25 atoms with the same input data as given in section 3.2, except the first shell atom positions. The distortions are performed according to the normal vibration modes. This does not suggest an effect of vibration in the XANES or EXAFS but it is the only compatible distortion. The directions of the atom shifts are described in figure 5.

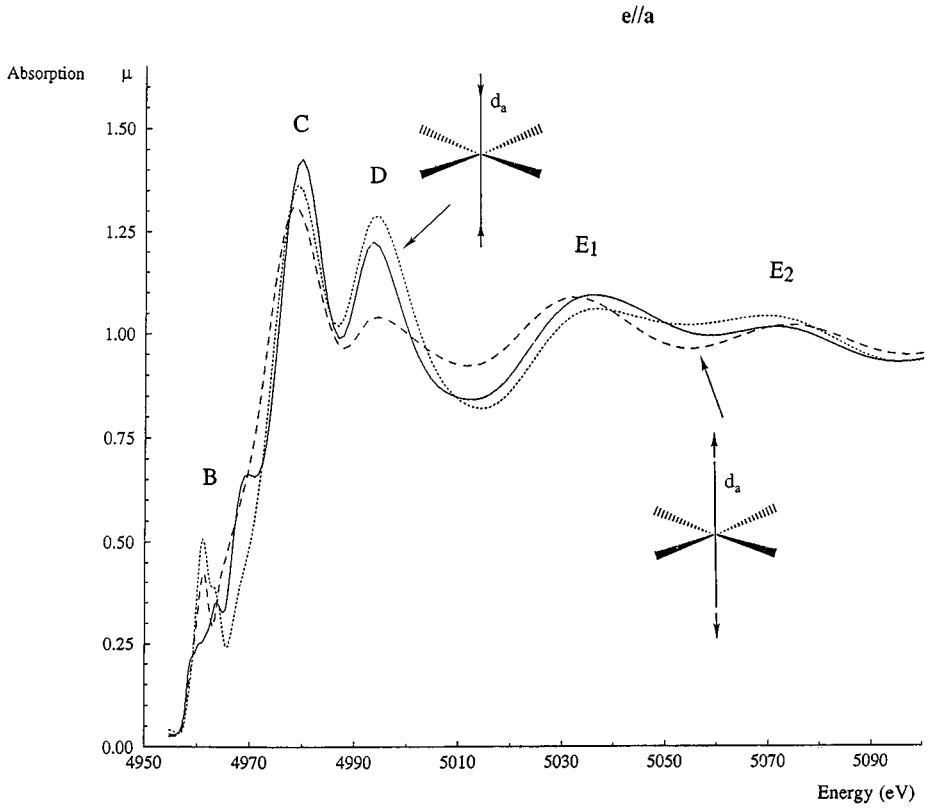

Figure 7. Calculated absorption of rutile TiO_2, with polarization perpendicular to the *c* axis. Solid line: rutile TiO_2 without distortion. Dotted line: reduction of the axial bond lengths. Dashed line: increasing of the axial bond lengths.

5. The TiO_2 absorption with geometry distortions

We performed several types of displacement for the six atoms of the first shell (0.1 Å shift of the oxygen atoms). These displacements are symmetric or antisymmetric according to the rutile TiO_2 group [45]. We determined the 21 elementary vibration modes but in this paper, we will show only the distortions which are related to the other rutile compounds. In other words, we made three kinds of distortion: modifications of the length of axial and equatorial bonds and variation of the equatorial angle (along the *c* axis). For a given polarization ($e \parallel c$ or $e \perp c$), the absorption of TiO_2 is calculated with the increase of the length or of the equatorial angle and afterwards it is calculated with the opposite case (i.e., the decrease of the length or angle). These two spectra are compared with the absorption of equilibrium rutile TiO_2 as a reference.

First, let us begin with the shifts of the axial oxygen into the axial distances Ti–O_{ap}:d_a.

5.1. Displacement of the axial oxygen atoms

The results of the absorption are shown in figures 6 and 7 respectively for the polarizations parallel and perpendicular to *c*.

In figure 6, the magnitude of the XANES structure C decreases when d_a decreases (dotted line). This effect is enhanced when the atoms are moved away from the central titanium (dashed line); the other structures are not really perturbed by this modification.

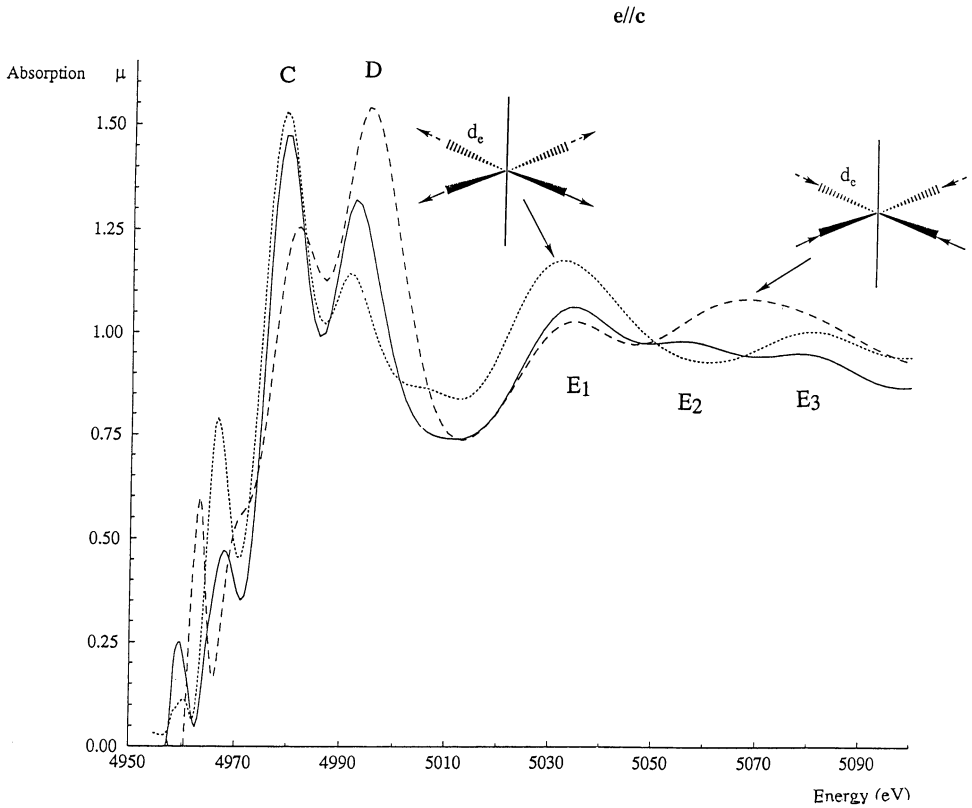

Figure 8. Calculated absorption of rutile TiO_2, with polarization parallel to the *c* axis. Solid line: rutile TiO_2 without distortion. Dotted line: four equatorial oxygen are moved away from central titanium by 0.1 Å. Dashed line: four equatorial oxygens are brought nearer to central titanium 0.1 Å.

The changes are more numerous in the case of the polarization perpendicular to *c* (figure 7). The reduction of the C structure is similar to the polarization parallel to *c* except smaller. For the structure D, the reduction of the distance yields the opposite effect (increase) on the amplitude. We can note a reduction of the amplitude of D when d_a increases; the change of the intensity is not symmetric when d_a is decreased. In contrast, the variation of the intensity is symmetric for the EXAFS structures at higher energies. The evolution of these structures is larger for the polarization perpendicular to *c*. We can explain this difference between the two polarizations as follows: the variation of the length of the axial distance is not detected following the polarization parallel to *c*, because the displacement is perpendicular to *c*. Nevertheless, these results yield information about the absorption structures connected to these axial atoms and also to the nature of the scattering. If there is no change parallel to the *c* axis, we can conclude that the scattering is single along the polarization perpendicular to the *c* axis.

Concerning structure C, it is perturbed in both cases. So, it can be concluded that the axial oxygen contributes to the multiple scattering.

5.2. Displacement of the equatorial oxygen along the linkage

In order to understand the multiple scattering contribution, we moved the equatorial oxygen by a value of 0.1 Å off the initial position along the linkage.

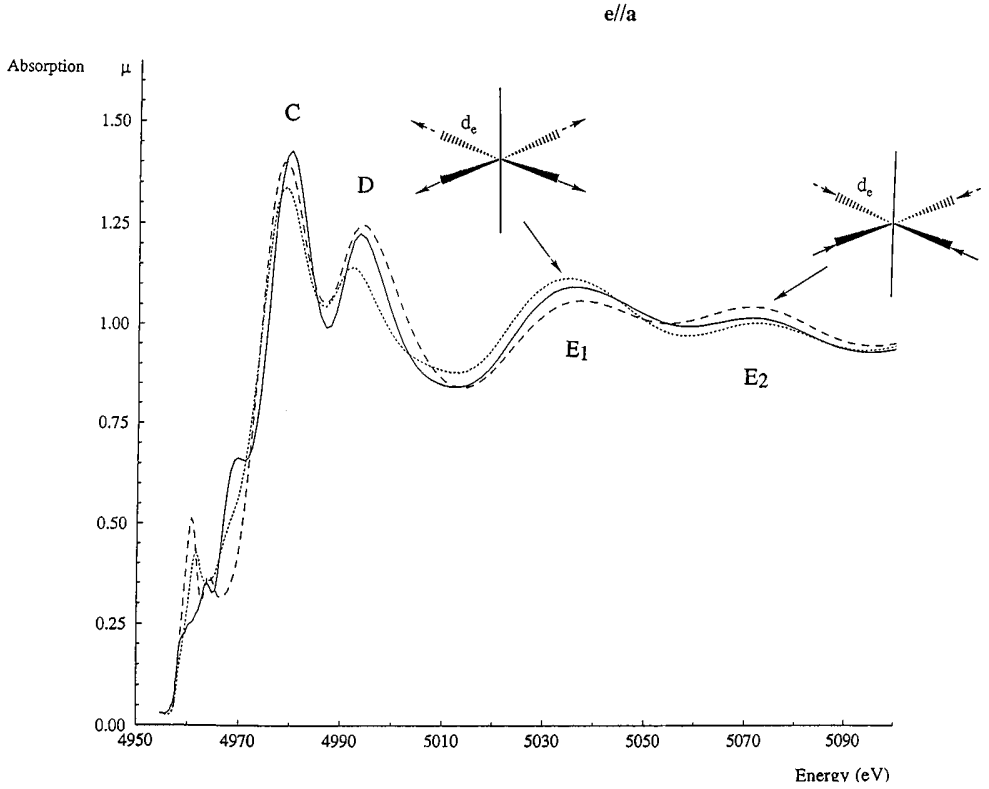

Figure 9. Calculated absorption of rutile TiO_2, with polarization perpendicular to the c axis. Solid line: rutile TiO_2 without distortion. Dotted line: four equatorial oxygens are moved away from central titanium by 0.1 Å. Dashed line: four equatorial oxygens are brought nearer to central titanium 0.1 Å.

Figures 8 and 9 show the absorption spectra when the equatorial oxygens are moved along the linkage following the polarization parallel and perpendicular to c respectively. For the polarization perpendicular to c, for all peaks, except the first XANES structure (C), when the equatorial length is increased or decreased, the magnitude of the structure evolves in the opposite direction.

In figure 8 ($e \parallel c$), in contrast to the other polarization ($e \perp c$), the modifications are very large for the XANES and EXAFS structures. For the structure C, as we deduce from all the pictures, this is the only case where its amplitude shows an increase for a TiO bond length increase (the oxygen are moved away from the central titanium), but a decrease for the opposite case (when the oxygen are moved closer to the central titanium). As a matter of fact, the changes of the structures D and the EXAFS structures are very asymmetric. Moreover, it is worth noticing that changes are not linear as they are not equal in absolute terms when bond length is increased and decreased. The variation of the amplitude of C for both polarizations ($e \parallel c$ and $e \perp c$) shows that there is a contribution of the axial oxygen in the scattering of the equatorial oxygen atoms.

The first and third EXAFS structures named E_1 and E_3 are unchanged. Indeed, we observed that these structures are not perturbed when we took off the four equatorial oxygen atoms [40, 46]. In fact, only the second EXAFS structure E_2 exhibits a decrease of its amplitude when one of the several equatorial oxygens are removed. So, these results show that the

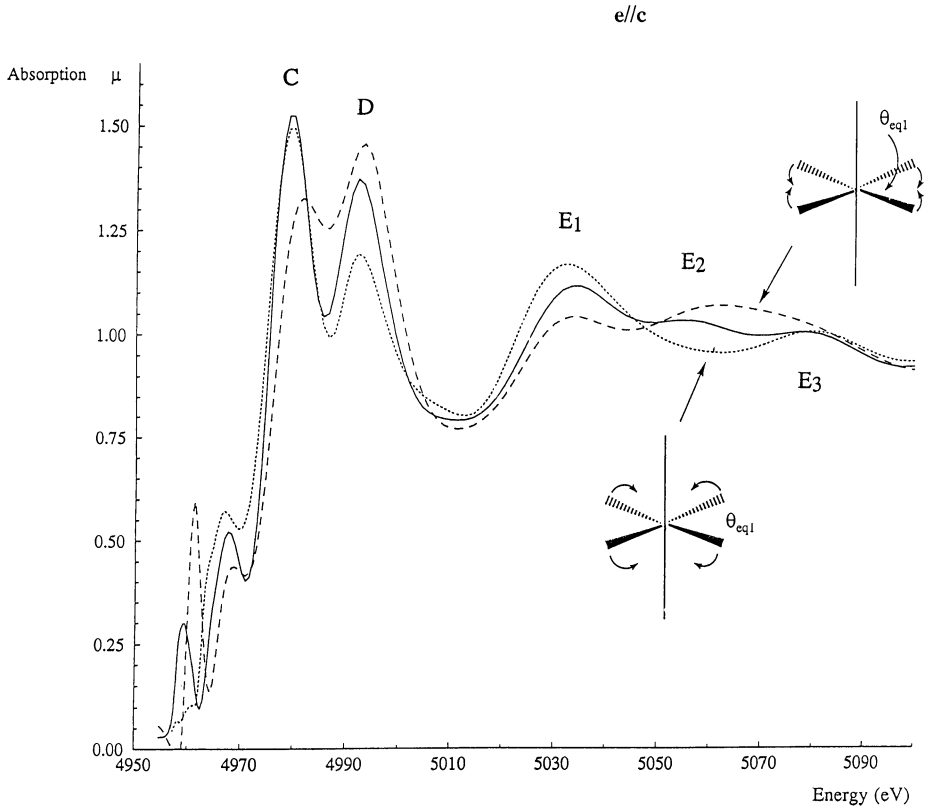

Figure 10. Calculated absorption of rutile TiO_2, with polarization parallel to the *c* axis. Solid line: rutile TiO_2 without distortion. Dotted line: increase of the O_{eq}–$\hat{T}i$–O_{eq} angle along the *c* axis. Dashed line: reduction of the O_{eq}–$\hat{T}i$–O_{eq} angle along the *c* axis.

oxygen atoms take part in the scattering only for E_2 and not for E_1 and E_3. Really, for the distortions along the equatorial linkage, this structure E_2 is not suppressed as appears in figure 8. E_2 is shifted towards the low energies when the equatorial oxygen atoms are moved away from the central titanium. This effect yields an increase of the E_1 amplitude. In the same way, the increase of E_3 results from the shift of E_2 towards higher energies, if the four oxygens are brought nearer the central atom.

5.3. Displacement of the equatorial oxygen perpendicular to the Ti–O bond

Let us shift the equatorial oxygen perpendicular to the Ti–O bond. This transformation yields a reduction or increasing of the equatorial angle along the *c* axis. The effects on the absorption are shown in figures 10 and 11 for the polarization parallel and perpendicular to the *c* axis respectively. Like case 5.2 (displacement along the linkage) except for the C structure (which shows a decrease for both distortions), the other structures exhibit a decrease or increase of their amplitudes for a given distortion and the opposite one respectively. The changes of the absorption are smaller for the perpendicular polarization, compared to the results for the other polarization. We conclude that the increase of the amplitude of E_1 or E_3 arises from the shifting of E_2 towards lower energies for E_1 and higher energies for E_3.

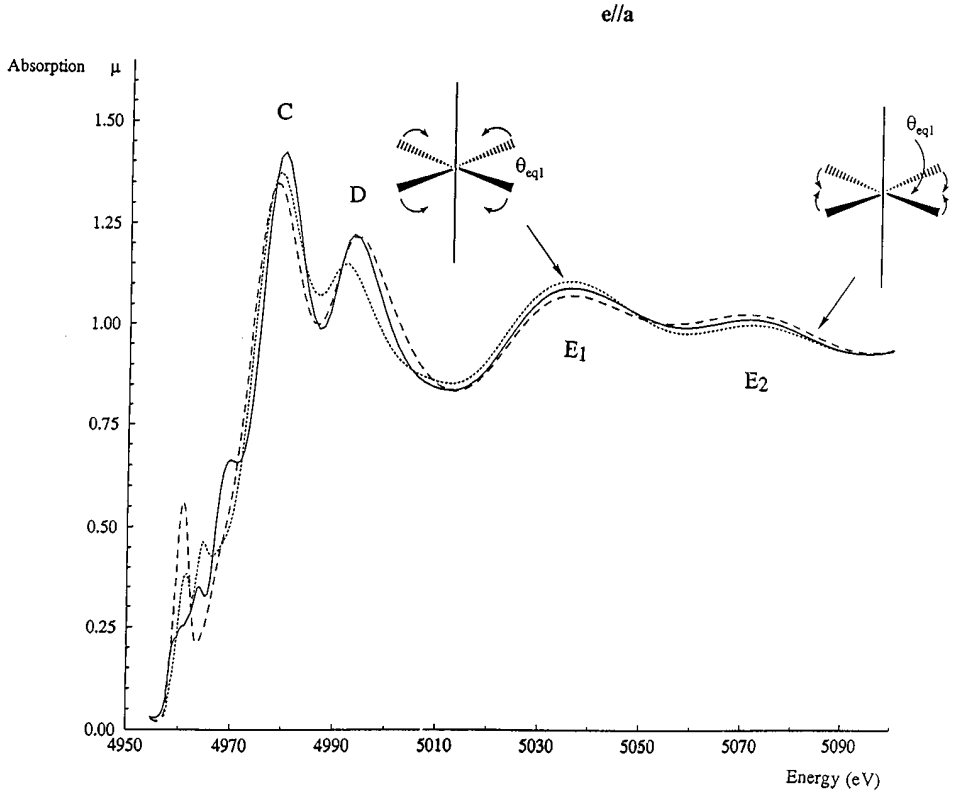

Figure 11. Calculated absorption of rutile TiO_2, with polarization perpendicular to the c axis. Solid line: rutile TiO_2 without distortion. Dotted line: increase of the O_{eq}–$\hat{T}i$–O_{eq} angle along the c axis. Dashed line: reduction of the O_{eq}–$\hat{T}i$–O_{eq} angle along the c axis.

These results confirm that the XANES and EXAFS structures C and E_2 are connected to the multiple scattering with a large contribution from the equatorial oxygen atoms and a smaller one from the axial atoms.

Generally, the variation of amplitudes are relatively less important in the case of a perpendicular shift than for the shift of the oxygen along the linkage, the polarization being the same. We can explain the amplitude difference between the absorption in figure 8 where the oxygen atoms are shifted in a parallel direction to the linkage and the amplitude of figure 10 where the oxygen atoms are shifted in a perpendicular direction to the linkage (the difference in the amplitudes of the absorption of figure 8 are higher than the ones in figure 10). For that, we may consider a difference due to the symmetry of the scattering coming from another atoms like the neighbouring titanium (Ti at $\pm c$) in addition to the axial and equatorial oxygen atoms. The titanium and oxygen atoms in the equatorial plane form the Ti0–O_{eq}–Ti2O_{eq} rhombus as in figure 12(*a*). For the absorption in figure 8, the rhombus recalled previously is not symmetric along the c axis (figure 12(*b*)); the Ti0–O_{eq} distances are greater than the Ti2–O_{eq} ones. This determines the symmetry of the scattering towards the central titanium. In the second case (figure 12(*c*)), the shift of the oxygen atoms is produced perpendicularly to the linkage, but the rhombus is still symmetric along the c axis compared with the rhombus of case (*a*) in figure 12. This effect would yield less modification of the amplitude of the different structures (figure 10).

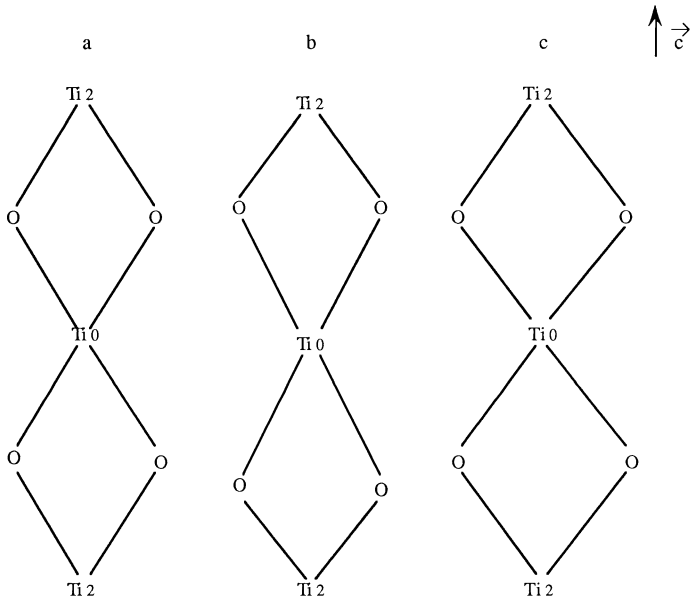

Figure 12. Equatorial plane (110) in the rutile TiO_2 structure: (*a*) rutile TiO_2 for comparison. (*b*) Distortion of the equatorial distances (d_e). (*c*) Distortion of the equatorial angle (θ_{eq1}).

6. Conclusion

In this work, we have investigated the importance of the geometry of the rutile structure in the x-ray edge absorption spectrum. We used the well known rutile compound titanium dioxide as a reference, in order to understand the connections between the XANES structures and atomic arrangement when weak distortions of the geometry into the first shell atoms are performed.

In this paper, we show the variations of the x-ray absorption spectrum with the variation of the axial and equatorial bond length (d_a and d_e) on one hand, and with the variations of the O_{eq}–$\hat{\text{Ti}}$–O_{eq} angle (θ_{eq1} along the *c* axis) on the other hand. With these results, we show that the increase in amplitude of the structure named D is connected to the reduction of the distance d_a. The change is smaller for polarization parallel to *c* than for the perpendicular one because the apical bonds are perpendicular to *c*.

If the value of d_e is modified, the magnitudes of C, D are perturbed and E_1, E_3 also. The amplitude of D decreases when the oxygen atoms are moved away from the central atoms. The variation of amplitude of E_2 is in fact a shift of this structure towards the low energies when the equatorial lengths are increased. The same effect is produced when the O_{eq}–$\hat{\text{Ti}}$–O_{eq} angle along the *c* axis is opened. The shift of the E_2 structure is in fact the cause of the main magnitude variation of the structures E_1 and E_3. As a matter of fact, these last structures are not connected to the changes of positions of the equatorial oxygen atoms.

D has its amplitude more perturbed than the other XAS structures when the four oxygen are moved slightly, for the two polarizations. This shows that there is a multiple scattering for this structure with axial and equatorial oxygen atoms.

On the other hand, we may anticipate or understand the evolution of the x-ray absorption structures of the spectra for the other rutile compounds in which the distances d_a and d_e are larger and θ_{eq} is smaller than these ones for the titanium dioxide TiO_2, for example the manganese difluoride MnF_2 ($d_a = 2.10$ Å; $d_e = 2.13$ Å and $\theta_{eq} = 78^\circ$ [22]) or the case

in which θ_{eq} is larger and d_a and d_e are smaller e.g., vanadium dioxide VO_2 ($d_a = 1.90$ Å; $d_e = 1.95$ Å and $\theta_{eq} = 82^\circ$ [47]).

Furthermore, we could use as well these results and conclusions for titanium dioxide which exists under other crystal structures than the ones presented in this paper. The case where the equatorial oxygen atoms are shifted out of the equatorial plane and the axial oxygen atoms are moved away from the central titanium is a real example: the titanium dioxide in the anatase structure (space group $I4_1/amd$ (D_{4h}^{19}) [32, 48, 49]). Even more, other irregular structures can be investigated, like the monoclinic vanadium dioxide (space group $P2_1/c$ [50]): the central vanadium is shifted from the initial position of the rutile structure. This will be the subject of future investigations.

Acknowledgment

We are very grateful to Professor J J Rehr for his advice.

References

[1] Faisant P 1978 *Thesis* Claude Bernard Lyon I
[2] Zaldo C, Galán Vioque J, Bausá L E and García Solé J 1991 *Phys. Status Solidi* a **127** 335–40
[3] Muñoz-Paez A and Justo A 1995 *Nucl. Instrum. Methods Phys. Res.* B **97** 11–15
[4] Le Granvalet-Mancini M 1994 *Thesis* Physico-chimie du Solide, Université de Nantes
[5] Grunes L A 1982 *Thesis* Cornell University
[6] Waychunas G A 1987 *Am. Mineral.* **72** 89–101
[7] Poumellec B, Cortès R, Tourillon G and Berthon J 1991 *Phys. Status Solidi* b **164** 319–26
[8] Locock A, Luth R W, Cavell R G, Smith D G W and Duke M J M 1995 *Am. Mineral.* **80** 27–38
[9] Beaurepaire E, Lewonczuc S, Ringeissen J, Parlebas J C, Uozumi T, Okada K and Kotani A 1993 *Europhys. Lett.* **22** 463
[10] Kizler P 1992 *Phys. Lett.* A **172** 66–76
[11] de Groot F M F, Faber J, Michiels J J M, Czyzyk M T, Abbate M and Fuggle J C 1993 *Phys. Rev.* B **48** 2074–80
[12] Poumellec B, Durham P J and Guo G Y 1991 *J. Phys.: Condens. Matter* **3** 8195
[13] Brydson R, Sauer H, Engel W, Thomas J M, Zeitler E, Kosugi N and Kuroda H 1989 *J. Phys.: Condens. Matter* **1** 797
[14] Vvedensky D D, Saldin D K and Pendry J B 1986 *Comput. Phys. Commun.* **40** 421–40
[15] Durham P J, Pendry J B and Hodges C H 1982 *Comput. Phys. Commun.* **25** 193–205
[16] Borgias B A, Cooper S R, Yun Bai Koh and Raymond K N 1984 *Inorg. Chem.* **23** 1009–16
[17] Ruiz-López M F and Muñoz-Páez A 1991 *J. Phys.: Condens. Matter* **3** 8981
[18] Borh F, Ruiz-López M F and Muñoz-Páez A 1993 *Catal. Lett.* **20** 59
[19] Natoli C R, Benfatto M and Doniach S 1986 *Phys. Rev.* A **34** 4682
[20] Natoli C R and Benfatto M 1986 *Journal Physique Coll.* **12** C8 11–23
[21] Wu Z Y, Ouvrard G and Natoli C R 1997 *J. Physique Coll.* **7** C2 199–201
[22] Dufek P, Schwarz K and Blaha P 1993 *Phys. Rev.* B **48** 12 672–81
[23] Soldatov A V, Stekhin I E, Kovtun A P and Bianconi A 1994 *J. Phys.: Condens. Matter* **6** 9817–24
[24] Rehr J J, Mustre de Leon J, Zabinsky S I and Albers R C 1991 *J. Am. Chem. Soc.* **113** 5135
[25] Van Meersche M and Ferneau-Dupont J 1984 *Introduction à la Cristallographie et à la Chimie Structurale* (Louvain Pa Neuve: Peeters)
[26] Bariand P, Cesbron F and Geffroy J 1978 *Les Mineraux Leurs Gisements, Leurs Associations* vol 2 (Paris: BRGM)
[27] Medvedeva N I, Zhukov V P, Khodos M Ya and Gubanov V A 1990 *Phys. Status Solidi* b **160** 517–27
[28] Svane A and Antoncik E 1987 *J. Phys. Chem. Solids* **48** 171–80
[29] Sorantin P I and Schwarz K 1992 *Inorg. Chem.* **31** 567
[30] Blanchin M G and Vicario E 1977 *J. Appl. Cryst.* **10** 228
[31] Fahmi A, Minot C, Silvi B and Causá M 1993 *Phys. Rev.* B **47** 11 717
[32] Cromer D T and Herrington K 1955 *J. Am. Chem. Soc.* **77** 4708–9
[33] Dagg C, Tröger L, Arvanitis D and Baberschke K 1993 *J. Phys.: Condens. Matter* **5** 6845

[34] Durham P J 1988 *X-Ray Absorption: Principles, Applications, Techniques of EXAFS, SEXAFS and XANES* vol 92, ed D C Koningsberger and R Prins (New York: Wiley) pp 52–84
[35] Mustre de Leon J, Rehr J J, Zabinsky S I and Albers R C 1991 *Phys. Rev.* B **44** 4146
[36] Loucks T 1967 *Augmented Plane Wave Method (Frontiers in Physics)* (New York: Benjamin)
[37] Rehr J J and Albers R C 1990 *Phys. Rev.* B **41** 8139–49
[38] Zabinsky S I, Rehr J J, Ankudinov A, Albers R C and Eller M J 1995 *Phys. Rev.* B **52** 2992–3009
[39] CNRS–CEA–NEAC 1992 *LURE Guide Technique* (Orsay: LURE)
[40] Jeanne-Rose V 1996 *Thesis* Chimie, Université Paris Sud XI
[41] Brydson R, Vvedensky D D, Engel W, Sauer H, Williams B G, Zeitler E and Thomas J M 1988 *J. Chem. Phys.* **92** 962–6
[42] Aïfa Y, Poumellec B, Jeanne-Rose V, Cortès R, Vedrinskii R V and Kraizman V L 1996 *J. Physique IV 9th Int. Conf. on X-Ray Absorption Fine Structure (Grenoble, 1996)* **2** 217–18
[43] Aïfa Y 1996 *Thesis* Chimie, Université Paris Sud XI
[44] Herman F and Skillman S 1983 *Atomic Structure Calculations* (Englewood Cliffs, NJ: Prentice-Hall)
[45] Jaffé H H and Orchin M 1965 *Symmetry in Chemistry* (New York: Wiley)
[46] Jeanne-Rose V, Aïfa Y and Poumellec B 1996 *9th Int. Conf. on X-Ray Absorption Fine Structure (Grenoble, 1996) J. Physique IV* **2** 221–2
[47] Westman S 1961 *Acta Chem. Scand.* **15** 217
[48] Henry N F M and Lonsdale K 1969 *International Tables for X-Ray Crystallography Vol I Symmetry Groups* (Birmingham: International Union of Crystallography)
[49] Horn M, Schwerdtfeger C F and Meagher E P 1972 *Z. Kristallogr.* **136** 273–81
[50] Andersson G 1956 *Acta Chem. Scand.* **10** 623–8